Transient Response Analysis of Inverter-based Microgrids under Unbalanced Conditions using Dynamic Phasor Model

Shuai, Zhikang; Peng, Yelun; Guerrero, Josep M.; Li, Yong; Shen, John Zheng

Published in:
IEEE Transactions on Industrial Electronics

DOI (link to publication from Publisher):
10.1109/TIE.2018.2844828

Publication date:
2019

Document Version
Accepted author manuscript, peer reviewed version

This article has been accepted for publication in a future issue of this journal, but has not been fully edited. Content may change prior to final publication. Citation information: DOI 10.1109/TIE.2018.2844828, IEEE Transactions on Industrial Electronics

Transient Response Analysis of Inverter-based Microgrids under Unbalanced Conditions Using Dynamic Phasor Model

Zhikang Shuai, *Senior Member*, *IEEE*, Yelun Peng, Josep M. Guerrero, *Fellow*, *IEEE*, Yong Li, *Senior Member*, *IEEE*, and Z. John Shen, *Fellow*, *IEEE*

***Abstract*— Microgrids (MGs) are often unbalanced due to the integration of single-phase generators, unbalanced loads and asymmetrical faults. To better analyze such a MG, this paper presents an approach to analyze the transient response for an inverter-based MG under unbalanced condition. The dynamic phasor (DP) concept is used for the MG modeling under stationary *abc* reference frame. First, the DP model of the inverter-based DG is developed. The influence of unbalanced conditions on the inverter including oscillations on dc side are considered in this paper. Then, the model of the network and loads is developed. Finally, all the sub-modules are combined on a time-variable system frequency to obtain the complete DP model of unbalanced MG.**

To validate the proposed approach, the DP method is applied to a MG test system with three-phase and single-phase DGs. Small signal analysis is carried out to derive the dominant modes and their influence on the system response. Simulation results from the DP model are compared against the detailed model built in MATLAB/SimPowerSystem. The results from load disturbances and asymmetrical faults are used to verify the DP model.

***Index Terms*—Inverter-based microgrid, unbalanced condition, dynamic phasor method, stability analysis.**

I. Introduction

With high penetration of renewable energy, the microgrid (MG) concept has been proposed for the efficient and flexible utilization of distributed generation (DG) [1]. Various kinds of DGs, such as photovoltaic (PV) systems and fuel cells are connected to MGs via power electronic inverters [2]. The inverter-based DGs with low-inertia are vulnerable to oscillation [3]. The inrush current and spike voltage caused by the large disturbance probably damage the power electronic devices and its storage capacitor. In addition, MG system usually operates under three-phase unbalanced condition [4-5] due to the integration of single-phase generators/loads and the occurrence of asymmetrical faults. The unbalanced configuration and susceptibility to oscillation will lead to significant challenges for the stable operation of MG.

The stability of a MG can be studied using the model created in commercial software such as PSCAD/EMTDC and Matlab/SimPowerSystem. The switching details of power electronic inverters are included in these models, which leads to a large computation burden. Furthermore, the switching models are discontinuous and thus difficult to be used for small-signal [6-8]and large-signal analyses [9]. Therefore, instead of the switching model, the dynamic average models are usually utilized for the numerical simulation and stability analysis.

The first step for stability analysis such as small-signal analysis and Lyapunov method [9] is to calculate a fixed equilibrium of dynamic model, followed by the linearization or calculation of energy function on the obtained equilibrium. Under balanced assumption, dynamic average model is transformed from the *abc*-frame into the synchronous rotating dq reference frame to obtain the fixed equilibrium [7-10]. However, the unbalanced operation of MG will produce an oscillating equilibrium and second harmonics of the state variables on dq reference frame. Thus, the model on *dq* reference frame is incapable of analyzing for the MG system under unbalanced condition. The sequence-component method has been used to analyze the electrical system under asymmetrical fault [2,11]. However, the sequence component model cannot fully present the three-phase unbalanced structure and parameters, such as single-phase DGs, unbalanced network and loads. Thus, this method is limited to analyze the systems with balanced structure [2].

Dynamic phasor (DP) method can describe the periodic varying signals using dc variables. A fixed equilibrium can be obtained from the DP model on *abc* reference frame, which allows a full presentation of different unbalanced condition. In [12], the small-signal stability of droop-controlled DG is analyzed by developing a character equation based on dynamics phasor method. The developed model is based on the balanced assumption and is equivalent as a single-phase system. Thus, the effect of unbalance on the transient response of inverter are not taken into account. The dynamic phasor modeling has also been used for the harmonics analysis of voltage source converter [13], stability analysis of AC machine [14] and high-voltage direct current (HVDC) systems [15]. In [16], the dynamic phasor method is used for modeling of radial distribution systems under unbalanced condition. The

Manuscript received February 09, 2018; revised, March 22, 2018; accepted May 29, 2018. This work was supported by the National Natural Science Foundation of China under Grant 51622702. (Corresponding author: Zhikang Shuai) and Hunan Provincial Innovation Foundation for Postgraduate under Grant CX2017B106 (Corresponding author: Yelun Peng).

Z. Shuai, Y. Peng, and Y. Li are with the College of Electrical and Information Engineering, Hunan University, Changsha 410082, China (e-mail: zhikangshuai@hotmail.com; pengyelun@163.com; yongli@hnu.edu.cn).

Josep M. Guerrero is with the Department of Energy Technology, Aalborg University, 9220 Aalborg, Denmark (e-mail: joz@et.aau.dk).

Z. J. Shen is with the Department of Electrical and Computer Engineering, Illinois Institute of Technology, Chicago, IL 60616 USA (e-mail: zjohnshen@gmail.com).

This article has been accepted for publication in a future issue of this journal, but has not been fully edited. Content may change prior to final publication. Citation information: DOI 10.1109/TIE.2018.2844828, IEEE Transactions on Industrial Electronics

distribution system with induction motor load and single-phase PV are connected to a stiff grid with constant system frequency. The complete DP model in [16] are built on the constant frequency, which cannot formulate the system with time-varying frequency such as microgrid. Therefore, the inverter-based DG that manipulates the frequency and voltage of electrical system has not been included in the distribution system [16]. The DP method proposed in [13-16] can only describe the periodical signal with constant frequency. However, in MG system, DGs cannot synchronize perfectly during the transient process [17]. The inverter-based DGs participate in the system frequency by means of the Phase-locked loops (PLL) or droop power controller. The frequency shift is slight but manipulates the power-angle relationships among DGs, which determines the power sharing and operating point of a complete system.

In [18], the DP method for time-varying frequency systems and multi-frequency system is proposed. Then, the proposed theory is applied to an aircraft system with two generators. However, the transient characteristic of inverter-based MG is different from those of generator-based electrical system. The control system and circuit topology of DG dominate the transient behavior of inverter-based MG. The modeling procedure and transient analysis of inverter-based MG under unbalanced condition has not been discussed in the papers mentioned above. To fill this gap, this paper extends the DP modeling to the inverter-based MG under unbalanced condition. The control system and the circuit topology of inverter-based microgrid under unbalanced condition are formulated in detail. Then, the effects of control parameters on the transient response of MG are discussed via eigenvalue analysis and numerical simulation, which guides the controller design of unbalanced microgrid.

The rest of the paper is organized as following. In Section II, the dynamic phasor concept based on time-varying frequency is presented. In Section III, the DP modeling procedure of inverter-based MG is developed, which includes three-phase DGs, single-phase DGs, unbalanced network and loads. Section IV presents a case study for a test system with two synchronverter-based DGs, and single-phase PV. Eigenvalue analysis is carried out to validate the capability of DP model for small-signal analysis. Simulation results are provided to show the accuracy of DP model. Section V presents the conclusion.

II. Dynamic Phasor Concept

The DP concept is a generalized averaging method to describe the time-domain quasi-periodic waveform. The DP based on time-varying fundamental frequency is presented in this section. For a time-domain waveform $x(\tau)$ [18], the Fourier expansion of this waveform in the moving window $\theta \in (\theta\text{-}2\pi, \theta]$ can be presented by the summation of its Fourier series as:

$$x(\tau) = \sum_{k=-\infty}^{+\infty} X_k(t)\,\mathrm{e}^{jk\theta} = \sum_{k=-\infty}^{+\infty} X_k(\mathrm{t})\,\mathrm{e}^{jk\omega t} \tag{1}$$

where ω is the variable system frequency and θ is the phase angle defined as:

$$\theta(\mathrm{t}) = \int_0^t \omega(\tau)d\tau \tag{2}$$

$X_k(t)$ is the Fourier coefficient in complex form, which can be defined as a kth DP. It is defined as follows:

$$X_k(t) = \frac{1}{2\pi}\int_{\theta-2\pi}^{\theta} x(\theta)e^{-jk\theta}d\theta = \langle x\rangle_k \tag{3}$$

$X_k(t)$ as the kth DP describes the kth harmonics of $x(\tau)$ in complex form. The width of window keeps constant with the change of the frequency ($\theta = 2\pi$), which makes the equation (1) always integrable. Therefore, this improved DP presented here can be utilized for the electrical system with time-variable frequency. Since the DPs of a quasi-periodic waveform are constant at steady state, the DP model can be linearized at steady state for small-signal analysis.

The main mathematical characters can be described as:

$$\begin{cases} \langle x+y\rangle_k = \langle x\rangle_k + \langle y\rangle_k = X_k(\mathrm{t}) + Y_k(\mathrm{t}) \\ \langle ax\rangle_k = a\langle x\rangle_k = aX_k(\mathrm{t}) \\ \langle xy\rangle_k = \sum_{l=-\infty}^{l=\infty}\langle x\rangle_{k-l}\cdot\langle y\rangle_l = \sum_{l=-\infty}^{l=\infty} X_{k-l}(\mathrm{t})\cdot Y_l(\mathrm{t}) \\ \left\langle \frac{dx}{dt}\right\rangle_k = \frac{d\langle x\rangle_k}{dt} + jk\omega\langle x\rangle_k = \frac{dX_k(\mathrm{t})}{dt} + jk\omega X_k(\mathrm{t}) \end{cases} \tag{4}$$

As the fundamental frequency ω is time-varying its mathematical description is essential and should be included in a complete DP model.

For a real time-domain waveform $x(t)$, its DPs also have the property as:

$$X_{-k}(\mathrm{t}) = X_k^*(\mathrm{t}) \tag{5}$$

where $X_k^*(\mathrm{t})$ is the complex conjugate of $X_k(\mathrm{t})$. Substituting (5) into (1), the real time-domain waveform can be written as:

$$x(t) = X_0(t) + \sum_{k=1}^{\infty}\{\mathrm{Re}[2X_k(t)e^{jkwt}]\} \tag{6}$$

It can be seen from the (6) that the real waveform can be presented by the DPs whose order $k \geqq 0$. In DP modeling, the numbers of DPs for a time-domain waveform are decided according to the accuracy requirement. For the balanced electrical system [12], the inverter model commonly contains fundamental component of DP for the variables in ac side and dc components of DP for the variables in dc side.

III. Dynamic Phasor Modeling of the Microgrid

In this section, the DP modeling for inverter-based microgrid is presented. The DP model of inverter-based microgrid is divided into the inverter-based DGs, network and load. At first, the DP models of three-phase DG and single-phase DG are developed. Then, the DP models of three-phase network and load are built. Considering the small-time constant of distribution lines, network model is described by algebraic equations. The DP model of a complete system is presented on the *abc* three-phase coordinate, which completely describes the load and network unbalances.

A. DP Model of the Three-Phase Inverter-Based DG

The DGs are commonly interfaced to the microgrid via the voltage source inverter. Fig.1 shows the block diagram of the synchronverter based DG. The ac side of the inverter consists of

This article has been accepted for publication in a future issue of this journal, but has not been fully edited. Content may change prior to final publication. Citation information: DOI 10.1109/TIE.2018.2844828, IEEE Transactions on Industrial Electronics

three-leg inverter, LC filter, and coupling inductors. The capacitors of LC filter are connected in Y-connection. Two fictitious capacitors $2C_{dc}$ are used to obtain a midpoint n' of the dc link, and thus do not physically exist. The energy resource and storage device of three-phase DGs can be approximated by an equivalent resistance R_{dc} and L_{dc} in series with an ideal voltage source, as illustrated in Fig. 1.

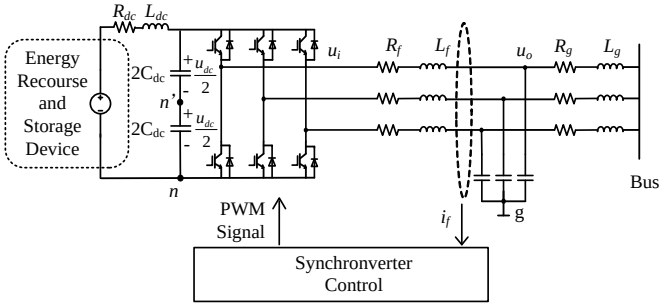

Fig. 1. Diagram of the inverter-based DG with synchronverter control.

The dynamic model of the dc side of the inverter-based DG can be written as:

$$L_{dc}\frac{di_{dc}}{dt}=u_{dc}^{*}-u_{dc}-R_{dc}i_{dc} \tag{7}$$

$$C_{dc}\frac{du_{dc}}{dt}=i_{dc}-i_{s} \tag{8}$$

where L_{dc} and R_{dc} denote the inductor and resistor respectively. u^{*}_{dc} is the voltage of ideal voltage source and u_{dc} is the voltage of input capacitor. i_{dc} and i_s are the output current from the ideal voltage source and input current of inverter, respectively. Considering the fundamental components of duty cycle, the relationship between the inject current i_s and filter current i_f on ac side can be written as:

$$i_{s}=\sum_{j=a,b,c}d_{j}i_{fj} \tag{9}$$

where d_j is the average duty cycle of PWM modulation.

The synchronverter that mimics synchronous generators is adopted here for the three-phase DG. Synchronverter control can enhance the virtual inertia and the dynamic stability of inverter-based DG [19]. When disturbances such as load changes or grid faults occur, synchronverter adjusts the angular frequency of output voltage spontaneously based on the virtual inertia provided by power controller, thereby maintaining the stability of microgrid.

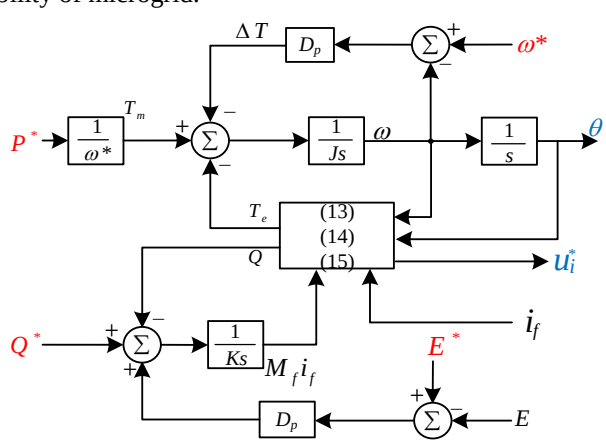

Fig. 2. Block diagram of synchronverter control.

The output current signals, i_f, are collected to the controller. The control part of synchronverter is presented in Fig.2. Where, E^* denotes the reference terminal voltage amplitude, ω^* is the reference frequency, and P^* and Q^* denote the reference active and reactive power, respectively.

The active power control loop and reactive power control loop can mimic the droop property of synchronous generator. The active power control equations that present the mechanical kinematic performance of machine are:

$$J\frac{d\omega}{dt}=\frac{P^{*}}{\omega^{*}}-T_{e}-D_{p}\left(\omega^{*}-\omega\right) \tag{10}$$

$$\frac{d\theta}{dt}=\omega \tag{11}$$

where J is moment of inertia and D_p denotes active damping coefficient. T_e is electromagnetic toque and ω is output angular frequency of synchronverter.

The reactive power control equation is:

$$\frac{dM_{f}i_{f}}{dt}=\frac{1}{K}\left[Q^{*}+D_{q}\left(E^{*}-E\right)-Q\right] \tag{12}$$

where D_q is the voltage-drooping coefficient, K is inertia coefficient related to D_q. M_f and i_f denote the virtual mutual inductance and rotor excitation current respectively, and $M_f i_f$ is treated as a dynamic state for the voltage control. The calculation of the reference terminal voltage u_{ij}, reactive power Q, the electromagnetic toque T_e and the amplitude of output voltage can be obtained as follow:

$$u_{ij}=\omega M_{f}i_{f}\sin\theta_{j}\,(j=\mathrm{a,b,c}) \tag{13}$$

$$Q=-\omega M_{f}i_{f}\,(i_{La}\cos\theta_{a}+i_{Lb}\cos\theta_{b}+i_{Lc}\cos\theta_{c}) \tag{14}$$

$$T_{\mathrm{e}}=M_{f}i_{f}\,(i_{La}\sin\theta_{a}+i_{Lb}\sin\theta_{b}+i_{Lc}\sin\theta_{c}) \tag{15}$$

$$E=\left[-\frac{4}{3}\left(u_{a}u_{b}+u_{a}u_{c}+u_{c}u_{b}\right)\right]^{1/2} \tag{16}$$

From (13), the averaging duty cycle d_j can be written as:

$$d_{i}=0.5+\frac{u_{i,j}}{u_{dc}^{*}} \tag{17}$$

The dynamic equation of the filter current can be presented as:

$$L_{f}\frac{di_{f,j}}{dt}=d_{j}u_{dc}-u_{o,j}-u_{gn} \tag{18}$$

Where, j denotes the phase (j=a, b, c), $u_{o,j}$ is the output voltage of LC filter, u_{gn} is the voltage difference between the neutral node g and the n point of dc side. Add the current equation (17) in each phase (j=a, b, c) up as follow:

$$\sum_{j=a,b,c}L_{f}\frac{di_{f,j}}{dt}=1.5u_{dc}+\sum_{j=a,b,c}u_{ij}-\sum_{j=a,b,c}u_{o,j}-3u_{gn} \tag{19}$$

For the three-phase three-leg inverter in Fig.1, there is no zero sequence current channel for the filter current $i_{f,j}$, the summation of the filter current i_f are equal to zero. Meanwhile, the reference voltage $u_{i,j}$ are three phase balanced, thus the summation of d_j are equal to zero as well. Therefore, the equation (19) can be rewritten as:

$$\sum_{j=a,b,c}u_{o,\mathrm{j}}=1.5u_{dc}-3u_{gn}=-3u_{gn'} \tag{20}$$

When the synchronverter is under balanced condition, the u_{gn}=0.5 u_{dc}. That means the neutral node g and the middle point of dc link n' are equipotential. Under unbalanced condition, there is a potential difference between the midpoint n' and node g, this midpoint to neutral voltage deteriorates the balance of

This article has been accepted for publication in a future issue of this journal, but has not been fully edited. Content may change prior to final publication. Citation information: DOI 10.1109/TIE.2018.2844828, IEEE Transactions on Industrial Electronics

output voltage. The terminal voltage to neutral node $u_{ig,j}$ can be presented as:

$$u_{ig,j} = d_j u_{dc} - 0.5 u_{dc} - \frac{1}{3}\sum_{j=a,b,c} u_{o,j} \tag{21}$$

The voltage unbalance of the connected bus causes the second harmonics of active power and reactive power. Due to the oscillation of active power, second harmonic of the dc voltage will appear which may damage the dc capacitor in long term.

B. Dynamic Phasor Model of the Inverter-based DG with Synchronverter control

In this point, the DP model of the synchronverter based DG is developed. The output current and voltage on the ac side contain ±1st fundamental frequency component, and the variables on dc sides consider the dc and ±2nd harmonic component. Because the harmonics of the measured signals in the controller can be filtered using low-pass filter, electromagnetic toque T_e, system frequency ω, and the $M_f i_f$ contain only dc components ($\langle\omega\rangle_0$ and $\langle Mfif\rangle_0$, $\langle T_e\rangle_0$ respectively). The -*k*th DPs are presented as the complex conjugate of *k*th DP using (5).

1) *DC side of the three-phase inverter:* The DP model of the dc side can be written as follow:

$$L_{dc}\frac{d\langle i_{dc}\rangle_0}{dt} = u_{dc}^* - \langle u_{dc}\rangle_0 - R_{dc}\langle i_{dc}\rangle_0 \tag{22}$$

$$C_{dc}\frac{d\langle u_{dc}\rangle_0}{dt} = \langle i_{dc}\rangle_0 - \sum_{j=a,b,c}[\langle d_j\rangle_{+1}\langle i_{fj}\rangle_{-1} + \langle d_j\rangle_{-1}\langle i_{fj}\rangle_{+1}] \tag{23}$$

$$L_{dc}\frac{d\langle i_{dc}\rangle_2}{dt} = -\langle u_{dc}\rangle_2 - R_{dc}\langle i_{dc}\rangle_2 - j2L_{dc}\langle\omega\rangle_0\langle i_{dc}\rangle_2 \tag{24}$$

$$C_{dc}\frac{d\langle u_{dc}\rangle_2}{dt} = \langle i_{dc}\rangle_2 - \sum_{j=a,b,c}\langle d_j\rangle_{+1}\langle i_{fj}\rangle_{+1} - j2C_{dc}\langle\omega\rangle_0\langle u_{dc}\rangle_2 \tag{25}$$

2) Control Part of the Synchronverter: The dynamic equations of power controller from (10-12) can be presented by using the DP equations as:

$$J\frac{d\langle\omega\rangle_0}{dt} = \frac{P^*}{\omega^*} - \langle T_e\rangle_0 - D_p\left(\omega^* - \langle\omega\rangle_0\right) \tag{26}$$

$$K\frac{d\langle M_f i_f\rangle_0}{dt} = Q^* + D_q\left(E^* - \langle E\rangle_0\right) - \langle Q\rangle_0 \tag{27}$$

where, the DPs of the electromagnetic toque $\langle T_e\rangle_0$ and the reactive power $\langle Q\rangle_0$ are presented as:

$$\begin{aligned}\langle T_e\rangle_0 &= \sum_{j=a,b,c}\langle M_f i_f \cdot i_{Lj}\cdot\sin\theta_j\rangle_0 \\ &= \sum_{j=a,b,c}(\langle M_f i_f\rangle_0\langle i_{Lj}\rangle_1^*\langle\sin\theta_j\rangle_1 + \langle M_f i_f\rangle_0\langle i_{Lj}\rangle_1\langle\sin\theta_j\rangle_1^*)\end{aligned} \tag{28}$$

$$\begin{aligned}\langle Q\rangle_0 &= \sum_{j=a,b,c}\langle\omega M_f i_f \cdot i_{Lj}\cdot\cos\theta_j\rangle_0 \\ &= \sum_{j=a,b,c}\left[\langle\omega\rangle_0\langle M_f i_f\rangle_0\langle i_{Lj}\rangle_1^*\langle\cos\theta_j\rangle_1 + \langle\omega\rangle_0\langle M_f i_f\rangle_0\langle i_{Lj}\rangle_1\langle\cos\theta_j\rangle_1^*\right]\end{aligned} \tag{29}$$

The 1st DPs of the reference output voltage u_{ij} of phase *j* (*j*=a, b, c) can be written as:

$$\langle u_{i,j}\rangle_1 = \langle\omega\cdot M_f i_f\cdot\sin\theta_j\rangle_1 = \langle\omega\rangle_0\langle M_f i_f\rangle_0\langle\sin\theta_j\rangle_1 \tag{30}$$

The DP of the output voltage to neutral node $u_{ig,j}$ can be presented as:

$$\langle u_{ig,j}\rangle_1 = \langle d_j\rangle_1\langle u_{dc}\rangle_0 - 0.5\langle u_{dc}\rangle_0 - \frac{1}{3}\sum_{j=a,b,c}\langle u_{o,j}\rangle_1 \tag{31}$$

The DP model of each there-phase inverter is modeled at its local frequency at first. The 1st DPs of the $sin\theta_j$ and $cos\theta_j$ in (29-30) at the fundamental angle $\theta = \omega t$ can be calculated as follow:

$$\langle\sin\theta_a\rangle_1 = \frac{1}{2\pi}\int_{\theta-2\pi}^{\theta}\frac{e^{j\theta}-e^{-j\theta}}{2j}e^{-j1\cdot\theta}d\theta = 0 - \frac{1}{2}j \tag{32}$$

$$\langle\sin\theta_b\rangle_1 = \langle\sin\theta_a\rangle_1 e^{-\frac{2}{3}\pi j}, \quad \langle\sin\theta_c\rangle_1 = \langle\sin\theta_a\rangle_1 e^{+\frac{2}{3}\pi j}$$

2) *LC filter and Coupling Inductor:*

The output LC filter and the coupling inductance DP model can be represented as follow:

$$L_f\left\langle\frac{di_{f,j}}{dt}\right\rangle_1 = \langle u_{ig,j}\rangle_1 - \langle i_{f,j}\rangle_1 R_f - \langle u_{o,j}\rangle_1 - j\langle w\rangle_0 L_f\langle i_{f,j}\rangle_1 \tag{33}$$

$$C_s\left\langle\frac{du_{o,j}}{dt}\right\rangle_1 = \langle i_{f,j}\rangle_1 - \langle i_{o,j}\rangle_1 - j\langle w\rangle_0 C_s\langle u_{o,j}\rangle_1 \tag{34}$$

$$L_g\left\langle\frac{di_{o,j}}{dt}\right\rangle_1 = \langle u_{o,j}\rangle_1 - \langle i_{o,j}\rangle_1 R_g - \langle u_{g,j}\rangle_1 - j\langle\omega\rangle_o L_g\langle i_{o,j}\rangle_1 \tag{35}$$

C. Dynamic Pharos Model of the Single-phase PV

The basic configuration of a single-phase PV is illustrated in Fig. 3. Single stage DC/AC inverter is used for energy conversion. The main elements of the single-stage PV are the PV array, input capacitor C, DC/AC inverter and L filter. The control system of the PV is presented in Fig. 4.

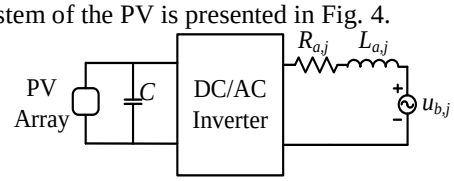

Fig. 3. Single-phase PV system.

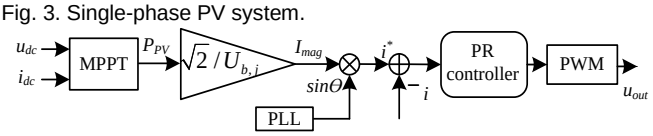

Fig. 4. Basic control of the PV system.

The control system consists of the maximum power point tracking (MPPT), phase-locked-loop (PLL), the current control loop with PR controller and pulse width modulation (PWM) module [16]. The amplitude of the reference output current of PV I_{mag} is calculated by equation: $I_{mag} = \sqrt{2}P_{pv}/U_{b,j}$, where P_{pv} is the PV array output power, $U_{b,j}$ is the RMS value of grid voltage. When the inverter is working under the unit power factor mode, the angle of the output current is provided by the PLL that measures the angel of bus voltage. In this paper, the effects of the MPPT and the dynamics of PLL are not taken into consideration.

Since the DPs of the reference output current i^* is in phase with DPs of the grid side voltage u_g, the DP of the i^* can be written as:

$$\langle i^*\rangle_1 = I_{mag}\cdot\langle u_{g,j}\rangle_1 / 2|U_{g,j}| \tag{36}$$

The PR controller is used to track the ac signal i^*. Defining the intermediate states x_1 and x_2 in the PR controller, the

This article has been accepted for publication in a future issue of this journal, but has not been fully edited. Content may change prior to final publication. Citation information: DOI 10.1109/TIE.2018.2844828, IEEE Transactions on Industrial Electronics

dynamic equations of the PR controller can be presented as [16]:

$$\begin{cases} \dfrac{d\langle x_1\rangle_1}{dt} = 0.5\left(\langle i_{ref}\rangle_1 - \langle i\rangle_1\right) - 2j\langle\omega\rangle_0\langle x_1\rangle_1 \\ \dfrac{d\langle x_2\rangle_1}{dt} = 0.5\left(\langle i_{ref}\rangle_1 - \langle i\rangle_1\right) \end{cases} \tag{37}$$

The 1st component of the DP for the output voltage u_{out} can be written as:

$$\langle u_{out}\rangle_1 = K_p\left(\langle i_{ref}\rangle_1 - \langle i\rangle_1\right) + K_r\left(\langle x_1\rangle_1 + \langle x_2\rangle_1\right) \tag{38}$$

Considering the 1st DP of the dynamic in the L filter, the DP equation of output current can be written as:

$$L_s\left\langle\frac{di_{\mathrm{out},j}}{dt}\right\rangle_1 = \langle u_{\mathrm{out},j}\rangle_1 - \langle i_{\mathrm{out},j}\rangle_1 R_f - \langle u_{\mathrm{b},j}\rangle_1 - j\langle\omega\rangle_0 L_s\langle i_{\mathrm{out},j}\rangle_1 \tag{39}$$

Substitute (38) into (39), the DP model of the single-phase PV consists of the (37) and (39).

D. Combined Model of DGs with Different Frequency

The angular frequency of the output voltage varies during the transient process. As the DP model of each DGs is defined on its local fundamental frequency. To connect DGs into a complete MG model, the output of each DG should be transformed into a common fundamental frequency. The relationship of the 1st DP of variable with different frequency ω is carried out as:

$$\langle x\rangle_{p,1} = e^{j\theta_{\mathrm{qp}}}\langle x\rangle_{\mathrm{q},1} \tag{40}$$

where $\theta_{qp} = \int(\omega_q - \omega_p)\,\mathrm{d}t$, $\langle x\rangle_{p,1}$ is the 1st DP of x with frequency ω_p, and $\langle x\rangle_{q,1}$ is the 1st DP of x with frequency ω_q.

One of the DG is selected as the master DG whose frequency is specified as the common fundamental frequency ω_{com}, and the rest of the DGs are the slave DGs. The master DG provides common fundamental frequency to all the subsystem of microgrid. As the fundamental frequency of PV is the frequency of the bus voltage measured by the PLL. Thus, PV should be taken as slave DG due to its incapability of frequency manipulation. The DPs of the output current of slave DGs are redefined on the common fundamental frequency as:

$$\langle i_{o,j}\rangle_{m,1} = e^{j\theta_{sm}}\langle i_{o,j}\rangle_{s,1}\ (j = a,b,c) \tag{41}$$

where $\theta_{sm} = \int(\omega_s - \omega_m)\,\mathrm{d}t$, subscripts m denotes the common fundamental frequency ω_{com}, s denotes salve DGs. The bus voltage should be transformed into the local frequency as the input of each DG, which can be written as:

$$\langle u_{g,j}\rangle_{s,1} = e^{j\theta_{ms}}\langle u_{g,j}\rangle_{m,1}\ (j = a,b,c) \tag{42}$$

where $\theta_{ms} = \int(\omega_m - \omega_s)\,\mathrm{d}t$.

When the MG is in grid-connected mode, the utility grid can be equivalent as the ideal voltage, whose voltage and frequency are constant.

E. DP Model of the Load

The load connected to microgrid is equivalent to the series connection of the resistors and inductance (RL load). The dynamic equations of the RL load connected at node i are:

$$L_{loadi,\mathrm{j}}\frac{di_{loadi,j}}{dt} = u_{bi,j} - R_{loadi,\mathrm{j}}i_{loadi,j},(\mathrm{j} = \mathrm{a,b,c}) \tag{43}$$

The DP model of RL loads are defined on the common fundamental frequency ω_{com}, which can be written as:

$$L_{loadi,j}\left\langle\frac{di_{loadi,j}}{dt}\right\rangle_1 = \langle u_{bi,j}\rangle_1 - \langle i_{loadi,j}\rangle_1 R_{loadi,j} - j\omega_{com}L_{loadi,j}\langle i_{loadi,j}\rangle_1 \tag{44}$$

F. DP model of the network

The DP model of network is developed using the algebraic equations in matrix form for a concise presentation. The network model is defined on the common frequency ω_{com}. It should be noticed that in three-phase framework, each phase of nodes should be defined individually. The series admittance between two nodes (p, q) is denoted by the 3×3 complex matrix $\mathbf{Y}_{\mathrm{pq}}$ as:

$$\mathbf{Y_{dq}} = \begin{bmatrix} \left(R_{pq,a} + j\omega_{com}L_{pq,a}\right)^{-1} & 0 & 0 \\ 0 & \left(R_{pq,\mathrm{b}} + j\omega_{com}L_{pq,\mathrm{b}}\right)^{-1} & 0 \\ 0 & 0 & \left(R_{pq,\mathrm{c}} + j\omega_{com}L_{pq,\mathrm{c}}\right)^{-1} \end{bmatrix}$$

where $R_{pq,j}$, $L_{pq,j}$ and ω_{com} denote the line resistance, inductance, and the common fundamental frequency respectively. For a network with l Buses, the network matrix can be presented by network matrix $\mathrm{Y_{net}} \in \mathrm{R}^{l\times l}$. Where the elements in this matrix $\mathbf{Y_{net}}$ are the $\mathrm{n}\times\mathrm{n}$ matrix ($\mathrm{n} \leqq 3$) denoted as follow:

$$\mathbf{Y_{net}}(\mathrm{p,q}) = \begin{cases} \sum_{i=1}^{i=l}\mathbf{Y_{pi}}, & if\ \ p = q \\ -\mathbf{Y_{pq}}, & if\ \ p \neq q \cap (\mathrm{p,q}) \in \lambda \\ \mathbf{O}, & else \end{cases}$$

where $\mathbf{O}$ denotes zero matrix. The set $\lambda=\{(i, j)\}$ denotes that there is a connection between the buses i and bus j through a distribution line. If a phase of line does not exist, the corresponding column and row should be zero quantity. To avoid the singularity of network matrix, these rows and columns should be deleted. After delete the zero columns and rows, the final form of network matrix $\mathbf{Y_{net}}'$ is developed. Thus, the network interactions can be presented by the admittances matrix $\mathbf{Y_{net}}$ based on Ohm's and Kirchoff's laws as:

$$\mathbf{i_o} - \mathbf{i_{load}} = \mathbf{Y_{net}}'\ \mathbf{u_b} \tag{45}$$

where $\mathbf{i_o}$, $\mathbf{i_{load}}$ and $\mathbf{u_b}$ denote the inject current vector, output load current vector and node voltage vector in complex form respectively as follow:

$$\mathbf{I_o} = \left[i_{o1,\mathrm{a}},\ i_{o1,\mathrm{b}},\ i_{o1,\mathrm{c}}, i_{o2,\mathrm{a}}, \cdots,\ i_{ol,\mathrm{c}}\right]^T,$$

$$\mathbf{I_{load}} = \left[i_{load1,\mathrm{a}},\ i_{load1,\mathrm{b}},\ i_{load1,\mathrm{c}}, i_{load2,\mathrm{a}}\cdots i_{load3,\mathrm{c}}\right]^T,$$

$$\mathbf{U_b} = \left[u_{b1,\mathrm{a}},\ u_{b1,b},\ u_{b1,c}, u_{b2,\mathrm{a}}, \cdots u_{bl,\mathrm{c}}\right]^T$$

The superscript T denotes the transposition of matrix. For the phases of a node that do not exist, the corresponding element in these vectors are deleted. If there is no DG connected to the phase a of node j, $i_{oj,a}$ equal to zero, and so does the $i_{loada,j}$. The node voltage of network can be calculated from (45) as:

$$\mathbf{u_b} = \mathbf{Y_{net}^{-1}}(\mathbf{i_o} - \mathbf{i_{load}}) \tag{46}$$

The node voltages of network are treated as the input for each subsystem. Finally, the complete DP model of microgrid can be

This article has been accepted for publication in a future issue of this journal, but has not been fully edited. Content may change prior to final publication. Citation information: DOI 10.1109/TIE.2018.2844828, IEEE Transactions on Industrial Electronics

obtained by combing the DP model of three-phase DGs, single-phase DGs, loads and network.

IV. Validation of the DP Model of Unbalanced MG

In this section, A 220 V, 50Hz test MG is built to validate the DP model result. As shown in Fig. 5, the test MG consists of two synchronverter-based DGs and one single-PV. Three unbalanced loads are connected to Bus 1-3 respectively. The parameters of DGs are shown in Table I, the parameters of network and load are shown in Table II. In the test system, two synchronverter-based DGs are equally rated. The parameters of two DGs are the same so that they share the power equally during transient process. The measured electromagnetic toque T_e, reactive power Q and magnitude of output voltage E pass through 2nd-order Butterworth low-pass filter to attenuate the effect of harmonics. The high-order filters have little effect on the dynamics of synchronverter due to the relatively large time constant of synchronverter controller.

There are totally 39 phasor equations to describe the dynamic behavior of the test system. The 1st phasors among the state variables will be separated into real and imaginary components. Therefore, 65 state variables are introduced into its DP model and eigenvalue analysis presents 65 eigenvalues.

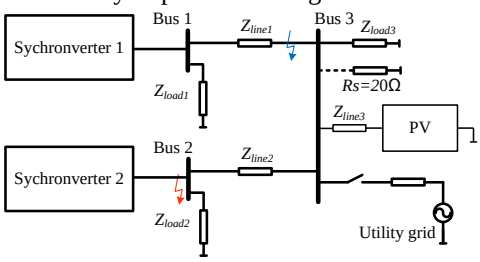

Fig. 5. Test system of the unbalanced MG system.

TABLE I. DG Parameters

Parameters	*Value*	*Parameters*	*Value*
P_n	10 kW	R_g	0.3 Ω
Q_n	5 kVar	C_{dc}	1mF
U_n	320 V	L_{dc}	1mH
D_p	20.28W/rad^2	R_{dc}	0.2 Ω
D_q	200 Var/V	u^*_{dc}	900V
τ_f	0.15s	P_{pv}	2 kW
τ_V	0.15s	K_p	3
L_f	3 mH	K_r	500
R_f	0.2 Ω	L_s	0.8 mH
C_f	35 μF	Rs	0.2 Ω
L_g	1.8 mH		

TABLE II. Network and Load Parameters

Parameters	*Value*		
	Phase a	*Phase b*	*Phase c*
Z_{line1}	0.6+0.002ωjΩ	0.6+0.002ωj	0.6+0.002ωj
Z_{line2}	0.75+0.0025ωjΩ	0.75+0.0025ωjΩ	0.75+0.0025ωjΩ
Z_{line3}	-	-	0.35+0.0013ωjΩ
Z_{load1}	25 Ω	40 Ω	40 Ω
Z_{load2}	30Ω	35Ω	30Ω
Z_{load3}	30+0.05ωjΩ	10+0.05ωjΩ	10+0.05ωjΩ

A. Eigenvalue Analysis and Sensitive Analysis

The dynamic stability of synchronverter-dominated MG and chosen values of droop coefficient have been discussed in [7]. The purpose of this section is to validate the capability of DP model for eigenvalue analysis. A fixed equilibrium of unbalanced MG can be obtained from the DP model. Thus, the linearized state matrix and eigenvalues of the microgrid can be derived without the balanced assumption.

The DP model of the test system is developed in MATLAB/Simulink environment. This DP model is linearized around the operating point using the MATLAB function "*linmod*," and eigenvalues are calculated by the function "*eig*". Finally, the eigenvalue spectrum of unbalanced MG can be obtained. As shown in Fig. 6, these eigenvalues can be divided into 3 clusters. The eigenvalues in cluster 3 are far from the right-half plane, while those in cluster 2 are widely distributed in the frequency region. The dominant eigenvalues in cluster 1 are close to the imaginary axis, and the participation analysis is applied to measure the coupling between the state variables and eigenvalues. From the participation analysis, the eigenvalues in cluster "3" relate to the output current in the coupling inductance of DGs. The eigenvalues in cluster "2" are largely sensitive to the state variables of LC filter, load and dc sides of variables. The dominant modes as shown in cluster "1" largely relate to the state variables of the power controller in the synchronverter and inner control loop of PV. The dominant low-frequency eigenvalues in cluster 1 and their related states are presented in Table III.

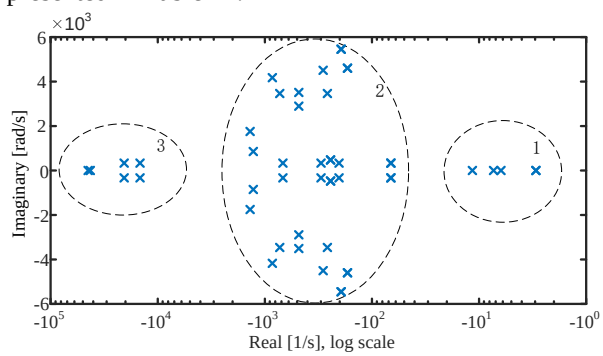

Fig. 6. Eigenvalue spectrum of the unbalanced MG.

TABLE III. Sensitive of Dominant Eigenvalues

Index	Eigenvalues	Related states	Participation
$\lambda_{1\text{-}2}$	-2.95± 7.75j	$\langle\theta_{12}\rangle_0$, $\langle\omega_1\rangle_0$	0.49, 0.22
λ_3	-6.23	$\langle M_f i_{f1}\rangle_0$, $\langle M_f i_{f2}\rangle_0$, $\langle\omega_1\rangle_0$, $\langle\omega_2\rangle_0$	0.26, 0.25, 0.24, 0.23
λ_4	-7.30	$\langle M_f i_{f2}\rangle_0$, $\langle M_f i_{f1}\rangle_0$, $\langle\omega_1\rangle_0$, $\langle\omega_2\rangle_0$	0.26, 0.25, 0.23, 0.23
λ_5	-11.52	$\langle M_f i_{f2}\rangle_0$, $\langle M_f i_{f1}\rangle_0$	0.46, 0.43
$\lambda_{6\text{-}7}$	-14.91±3.37j	$\langle x_2\rangle_1$	0.84
$\lambda_{8\text{-}9}$	-15.17±629.23j	$\langle x_1\rangle_1$	0.85

The sum of the participation factors on real and imaginary part is used to define the participation of 1st DPs. The eigenvalues $\lambda_{1\text{-}2}$ are low-frequency modes, which are sensitive to the active power controller of synchronverters. λ_3, λ_4 and λ_5 are highly related to the active and reactive power control. $\lambda_{6\text{-}7}$ and $\lambda_{8\text{-}9}$ are participated by the variables from the PR controller. Among these modes, $\lambda_{1\text{-}2}$ presents the low-frequency oscillation among the DGs, and $\lambda_{8\text{-}9}$ contribute to the medium-frequency oscillation produced by PR controller of PV.

This article has been accepted for publication in a future issue of this journal, but has not been fully edited. Content may change prior to final publication. Citation information: DOI 10.1109/TIE.2018.2844828, IEEE Transactions on Industrial Electronics

Since a cluster of low-frequency dominant modes from $\lambda_{1\text{-}2}$ to λ_5 are sensitive to the power controller of synchronverter. The parameters from power controller are selected to do eigenlocus analysis at first. Fig. 7(a) plots the eigenlocus with the change of inertia coefficient J and K_q. The low-frequency modes $\lambda_{1\text{-}2}$ move to the imaginary axis with the increase of J, which results in a poor-damped oscillation. Besides, the dominant modes from $\lambda_{1\text{-}2}$ to λ_5 are moving forward the imaginary axis with the increase of J and K_q, which slows down the transient response synchronverters. The Fig. 7(b) plots the eigenlocus of dominant modes with the change of frequency-droop and voltage-droop coefficient. With the decrease of droop coefficient, these modes move to toward imaginary axis. When D_p=2.04, the modes $\lambda_{1\text{-}2}$ pass through the imaginary axis and microgrid becomes unstable. The dominant modes $\lambda_{1\text{-}2}$ are less sensitive to the change of voltage-droop coefficient. However, the λ_3 is close to the imaginary axis when D_q is small, which slows down the transient response of synchronverter after perturbation. Therefore, both D_p and D_q should be large enough to make sure the transient performance of synchronverter. However, it should be noticed that relatively small D_p and D_q are necessary for an accurate power sharing and relative large J and K_q are needed to attenuate the harmonics of measured power produced by the switching and unbalanced condition.

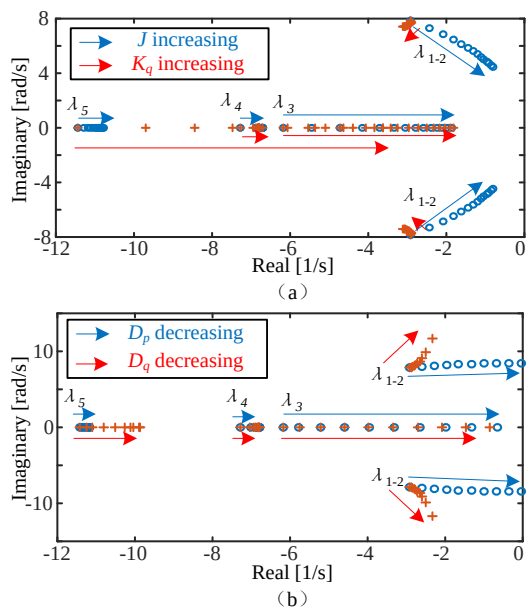

Fig. 7 Eigenlocus of the eigenvalue with the parameters change of power controller of synchronverter. (a) $3 \leqq J \leqq 10.2$, $9420 \leqq K_p \leqq 33912$, (b) $20.28 \geqq D_p \geqq 2.03$, $200 \geqq D_p \geqq 20$.

Besides, the pair of eigenvalues $\lambda_{8\text{-}9}$ have the smallest damping ratio, which will cause the medium-frequency oscillation of PV when disturbance occurs. To restrain such oscillation, it is suggested that the damping ratio ξ of medium-frequency modes should be larger than 0.1. Fig. 8 plots the eigenlocus of the $\lambda_{6\text{-}7}$ and $\lambda_{8\text{-}9}$ with the change of K_r and K_p of PR controller. For K_p=1, K_r decreasing from 2000 to 100, $\lambda_{6\text{-}7}$ and $\lambda_{8\text{-}9}$ move to the imaginary axis with the decrease of the K_r. For K_r=1000, K_p increasing from 1 to 19, $\lambda_{6\text{-}7}$ and $\lambda_{8\text{-}9}$ also move to the imaginary axis. The imaginary part of these dominant modes decreases slowly during the parameter change. Thus, increasing K_r or decreasing K_p results in a higher damping ratio for the medium-frequency modes, which eliminates this oscillation. However, it is to be noticed that a relatively large K_p is needed to eliminate the overshoot of current of PV.

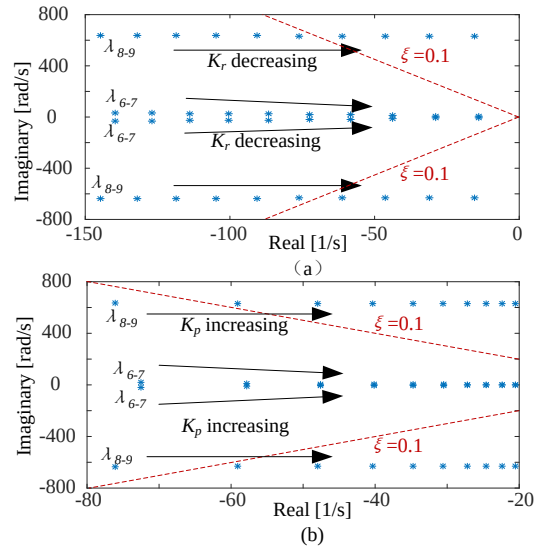

Fig. 8. Eigenlocus of the eigenvalue with the parameters change of PR controller. (a) $2000 \geqq K_r \geqq 100$, (b) $1 \leqq K_p \leqq 19$.

B. Simulation Results of the DP Model

In this section, the DP model results are validated against the high-fidelity switching model built in the MATLAB/ SimPowerSystem environment. The load disturbance and asymmetrical faults are designed to test the accuracy of the DP model. Besides, the transient response of MG with different control parameters is compared under different cases to investigate the influence of dominant modes on the transient performance of microgrid. First, the load disturbance is arranged to validate the low-frequency dynamics of the DP model. Second, an asymmetrical short-circuit fault is used to exam the medium-frequency and high-frequency dynamics. The third test is used to exam the performance of DP model under open-circuit fault.

a) Case study 1: Load Disturbance Test

In the first test, a disturbance in load of bus 3 was arranged. This requires the addition of a resistance load R_s in parallel to bus 3, as shown in Fig. 5. This disturbance was chosen to be 6.5 kW (R_s =20 Ω).

Fig. 9 (a) and (b) show the active and reactive power response of the synchronverter 1, respectively. The presentation of the DP for the active and reactive power is shown in the appendix. Due to the unbalanced condition of MG, the output power of the DGs contains second harmonics. As can be seen in (6), the combination of the DPs $\langle P_i \rangle_0 + 2|\langle P_i \rangle_2|$ and $\langle P_i \rangle_0 - 2|\langle P_i \rangle_2|$ corresponds to the upper and lower envelop of the active power in the switching model. $\langle Q_i \rangle_0 + 2|\langle Q_i \rangle_2|$ and $\langle Q_i \rangle_0 - 2|\langle Q_i \rangle_2|$ corresponds to the upper and lower envelop of the reactive power. The transient responses of the DP model match well with that of the switching model. Fig. 9 (c) depicts the frequency response of the test system. With the increase of the load, the frequency of the output voltage of synchronverter-based DG decreases.

This article has been accepted for publication in a future issue of this journal, but has not been fully edited. Content may change prior to final publication. Citation information: DOI 10.1109/TIE.2018.2844828, IEEE Transactions on Industrial Electronics

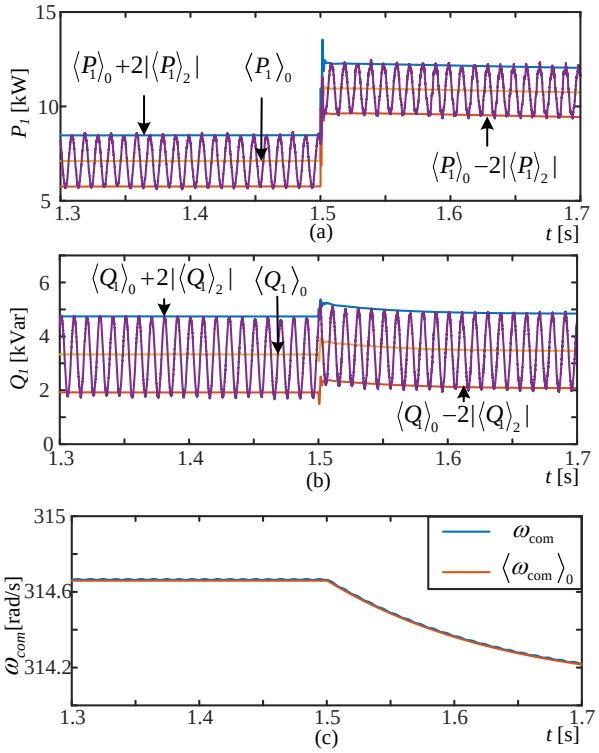

Fig. 9. System responses of the unbalanced microgrid with a 6.5-kW load step at bus 3. (a) Active response of the DG1, (b) Reactive response of the DG1, (c) Angular frequency response of the system.

In addition, the first test is used to investigate the sensitive of control parameters on the dominant dynamics of microgrid. The participation analysis in Section IV.A reveals that dominant modes majorly participate on the power controller of synchronverter. Among them, the low-frequency modes are highly related to output power. Therefore, the transient response of active and reactive power with different parameters of power controller is compared in the numerical simulation. Fig. 10 plots the combination of the DPs $\langle P_i\rangle_0+2|\langle P_i\rangle_2|$ and $\langle Q_i\rangle_0+2|\langle Q_i\rangle_2|$ when different inertia parameters are adopted. As shown in Fig. 10, a larger value of J and K_q slow down the transient response of synchronverter. The poor damped low-frequency oscillation is observed when a larger moment of inertia J is selected, which coincides with the sensitive analysis presented in Fig. 7(a). Fig. 11 illustrates the case when different droop coefficients are selected. Decreasing the voltage-drooping coefficient D_p introduces the low-frequency oscillation among DGs. Little effect of decreasing reactive-power coefficient on the low-frequency modes is observed. But it increases the response time of synchronverter.

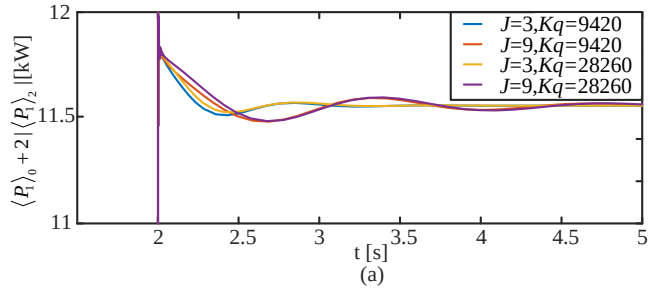

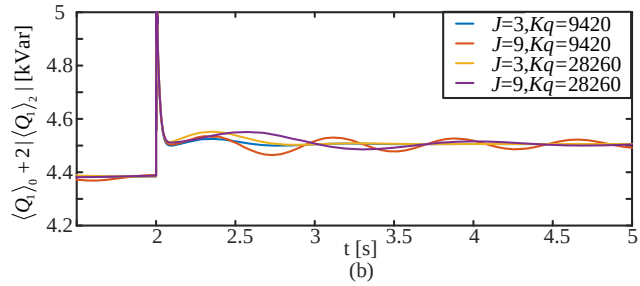

Fig. 10. The comparison of transient response of synchronverter with different inertia parameters.

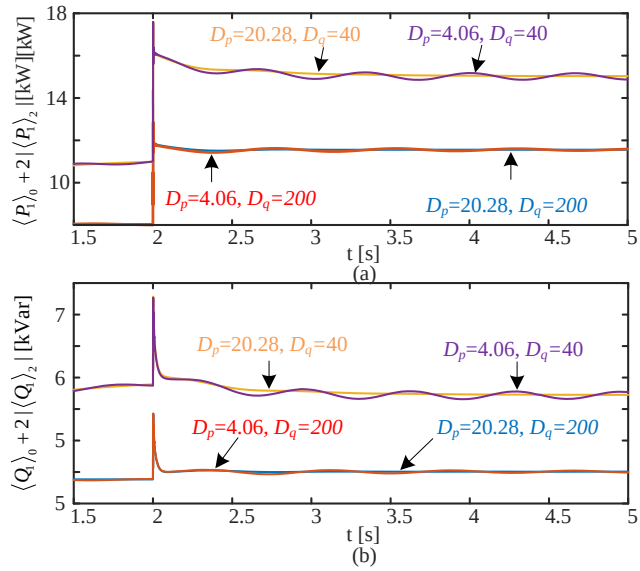

Fig. 11. The comparison of transient response of synchronverter with different droop coefficients.

b) Case study 2: Asymmetrical Short-circuit Fault Test

In the second test, two phase grounded fault with 1 Ω fault resistance is conducted in phase *a* and *b* of the bus 2 and is cleared after 5 cycles. The voltage of bus 2 and the fault response of DGs are presented in Fig. 12. As presented in Fig. 12 (a), the bus voltage at phase *a* and *b* dip to 47% of the value at steady state. The reference voltages of synchronverter-based DGs rise after this fault, which leads to the increase of the bus voltage at phase *c*. Fig. 12 (b) and (c) depict the output current of synchronverter-based DG 1 and DG2, respectively. In Fig. 12 (c), the output current of DG 2 is much larger than that of DG 1, due to that DG is closest to the fault location. As shown in fig. 12 (d), the output current of the single-phase PV increases abruptly and then decrease to the refence value due to the inner control. The capacitor voltage of the dc sides of synchronverter 2 is shown in Fig. 12(e). The DP model predicts the oscillation of dc capacitor voltage under asymmetrical fault. As the 2nd DPs describe the magnitude of the oscillation, the spike voltage predicted by DP model may not exist in switching model. But the DP model predict the worst scenario, which may destroy the capacitor under asymmetrical fault. Fig. 12 (f) shows the midpoint to neutral voltage. The waveforms of switching model are filtered by the low-pass filter to extract the fundamental component. A large oscillation with fundamental frequency appears during the asymmetrical faults, which imposes on the output voltage and deteriorates the voltage balance. The three-phase four-leg inverter or isolating

This article has been accepted for publication in a future issue of this journal, but has not been fully edited. Content may change prior to final publication. Citation information: DOI 10.1109/TIE.2018.2844828, IEEE Transactions on Industrial Electronics

transformer can mitigate node to ground voltage, but increase the cost and power loss of MG.

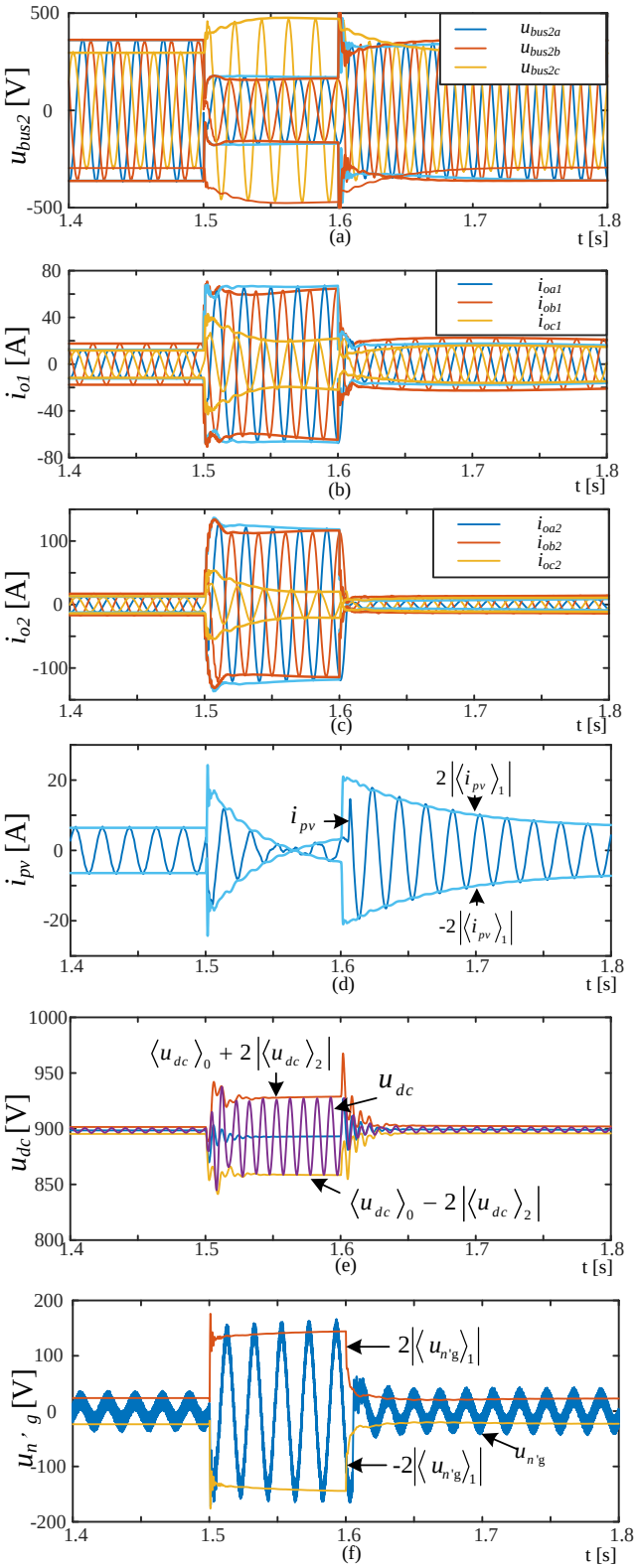

Fig. 12. System responses of the unbalanced microgrid when a single-phase short circuit occur at phase a of the bus 2. (a) Bus voltage of bus 2, (b) Output current of the DG1, (c) Output current of the DG2, (d) Output current of single-phase PV. (e) DC voltage of DG2, (f) DC midpoint to neutral voltage.

Then, the second test is used to validate the influence of the PR controller on the dominant medium-frequency modes $\lambda_{6\text{-}7}$ and $\lambda_{7\text{-}8}$ as presented in Table III. Since $\lambda_{6\text{-}7}$ and $\lambda_{7\text{-}8}$ are highly related to the PR controller of PV that manipulates the output current of PV, different K_p and K_r of PR controller are selected to investigate their influence on the output current of PV. The DP $2\langle i_{pv}\rangle_1$ are observed in the numerical simulation as shown in Fig. 13. Increasing K_r or decreasing K_p can attenuate the medium-frequency oscillation of output current and improve the transient response of PR controller. However, a small K_p may result in the overshoot of current.

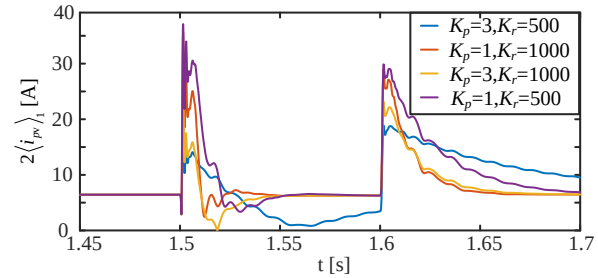

Fig. 13 Output current response of the PV with different parameters of PR controller.

c) Scenario 3: Asymmetrical Open-circuit Fault Test

In the third test, the open-circuit fault is conducted at distribution line between the bus 1 and bus 3 in phase *a*. The open-circuit fault is carried out by changing the element in network matrix. The line impedance of phase *a* is changed from $0.6+0.002\omega j\Omega$ to $1e^6\ \Omega$ at 1.5s. The output currents of DGs are presented in Fig. 14. The output current of DG1 in phase droops abruptly, and DG2 transmits more output current in phasor *a* for the power balance.

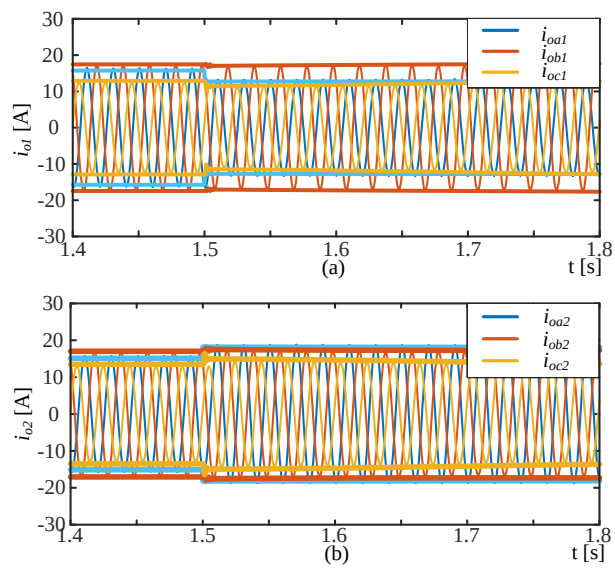

Fig. 14. System responses of the unbalanced microgrid when a single-phase open circuit occurs at distribution line between bus 1 and bus 3. (a) Output current of the DG1, (b) Output current of the DG2.

The simulation time of different scenarios is as presented in Table IV. The time-domain simulation of DP model runs much faster than that of the detailed model in MATLAB/SimPowersystem. Although the simulation time of the model relates to computing capability of computer, the simulation time from Table IV reflects the small computation burden of DP model. This is because the DPs describe the magnitude of the ac signals, the states in DP model vary slowly

This article has been accepted for publication in a future issue of this journal, but has not been fully edited. Content may change prior to final publication. Citation information: DOI 10.1109/TIE.2018.2844828, IEEE Transactions on Industrial Electronics

even when instantaneous quantities change abruptly. Therefore, large step time can be chosen for numerical simulation.

Table IV Simulation Time of Model

Scenarios	Time to be simulated	Switching model in *SimPowerSystem*	DP model
1	3s	2min48s	3s
2	5s	4min23s	5s
3	5s	4min12s	4s

V. Conclusion

This paper develops DP modeling procedure for inverter-based MG under unbalanced condition. Then the DP model is used to investigate the dynamic behavior of MG under unbalanced condition. The effects of control parameters on the transient behavior of MG are analyzed in detail. Several conclusions can be obtained：

1） The PR controller of single-phase introduces the medium-frequency dynamics with low damping ratio. The droop controller of synchronverter produces low-frequency oscillations among the DGs. The control parameters of DGs have significant influence on the transient performance of inverter-based MG.

2） For the three-phase three-leg inverter under unbalanced condition, dc midpoint to neutral voltage contains fundamental frequency component, which deteriorates the balance of output voltage. DC voltage fluctuation appears during the asymmetrical fault, which may damage the dc storage capacitor.

3） The DP model shows a good accuracy to capture the electromagnetic transient of unbalanced MG. The simulation time of DP model is much shorter than that of the switching model in MATLAB/SimPowerSystem.

The proposed DP modeling approach allows a complete presentation of unbalanced configuration and asymmetrical faults, which is suitable for the system design and analysis of inverter-based MG in large scale. Moreover, the DP model provides a fixed equilibrium for the MG before and after asymmetrical faults, which is necessary to construct Lyapunov function for stability analysis purpose. The future work includes the DP modeling of the three-phase DGs using the vector control, and transient stability analysis of the MG under asymmetrical faults.

VI. Appendix

The dc component and second harmonics of active and reactive power can be presented by using the output voltage and current of DG as:

$$\langle P\rangle_0 = \sum_{j=a,b,c}\langle i_{oj}u_{oj}\rangle_0 = \sum_{j=a,b,c}(\langle i_{oj}\rangle_1^*\langle u_{oj}\rangle_1 + \langle i_{oj}\rangle_1\langle u_{oj}\rangle_1^*) \quad \text{(A1)}$$

$$\langle P\rangle_2 = \sum_{j=a,b,c}\langle i_{oj}u_{oj}\rangle_2 = \sum_{j=a,b,c}\langle i_{oj}\rangle_1\langle u_{oj}\rangle_1 \quad \text{(A2)}$$

$$\begin{aligned}\langle Q\rangle_0 &= \langle i_{oa}(u_{ob}-u_{oc}) + i_{ob}(u_{oc}-u_{oa}) + i_{oc}(u_{oa}-u_{ob})\rangle_0 \\ &= (\langle i_{oa}\rangle_1^*\langle u_{ob}-u_{oc}\rangle_1 + \langle i_{oa}\rangle_1\langle u_{ob}-u_{oc}\rangle_1^* + \langle i_{ob}\rangle_1^*\langle u_{oc}-u_{oa}\rangle_1 \\ &\quad + \langle i_{ob}\rangle_1\langle u_{oc}-u_{oa}\rangle_1^* + \langle i_{oc}\rangle_1^*\langle u_{oa}-u_{ob}\rangle_1 + \langle i_{oc}\rangle_1\langle u_{oa}-u_{ob}\rangle_1^*)\end{aligned} \quad \text{(A3)}$$

$$\begin{aligned}\langle Q\rangle_2 &= \langle i_{oa}(u_{ob}-u_{oc}) + i_{ob}(u_{oc}-u_{oa}) + i_{oc}(u_{oa}-u_{ob})\rangle_2 \\ &= (\langle i_{oa}\rangle_1\langle u_{ob}-u_{oc}\rangle_1 + \langle i_{ob}\rangle_1\langle u_{oc}-u_{oa}\rangle_1 + \langle i_{oc}\rangle_1\langle u_{oa}-u_{ob}\rangle_1)\end{aligned} \quad \text{(A4)}$$

References

[1] Z. Shuai et al., “Microgrid stability: Classification and a review,” *Renewable & Sustainable Energy Reviews*, vol. 58, pp. 167–179, May 2016.

[2] Zhikang Shuai, C. Shen, X. Yin, Xuan Liu, and J. Shen, “Fault Analysis of Inverter-Interfaced Distributed Generators with Different Control Schemes,” *IEEE Trans. Power Deliv.*, vol. 33, no. 3, pp. 1223-1235, Jun. 2018.

[3] J. C. Vasquez, J. M. Guerrero, M. Savaghebi, J. Eloy-Garcia and R. Teodorescu, “Modeling, Analysis, and Design of Stationary-Reference-Frame Droop-Controlled Parallel Three-Phase Voltage Source Inverters,” *IEEE Trans. Ind. Electron.*, vol. 60, no. 4, pp. 1271-1280, Apr. 2013.

[4] E. Nasr-Azadani, C. A. Cañizares, D. E. Olivares and K. Bhattacharya, “Stability Analysis of Unbalanced Distribution Systems with Synchronous Machine and DFIG Based Distributed Generators,” *IEEE Trans. Smart Grid*, vol. 5, no. 5, pp. 2326-2338, Sept. 2014.

[5] X. Guo, W. Liu and Z. Lu, “Flexible Power Regulation and Current-Limited Control of the Grid-Connected Inverter Under Unbalanced Grid Voltage Faults,” *IEEE Trans. Ind. Electron.*, vol. 64, no. 9, pp. 7425-7432, Sept. 2017.

[6] E. A. A. Coelho *et al.*, “Small-Signal Analysis of the Microgrid Secondary Control Considering a Communication Time Delay,” *IEEE Trans. Ind. Electron.*, vol. 63, no. 10, pp. 6257-6269, Oct. 2016.

[7] Z. Shuai, Y. Hu, Y. Peng, C. Tu, and Z. J. Shen, “Dynamic Stability Analysis of Synchronverter-dominated Microgrid Based on Bifurcation Theory,” *IEEE Trans. Ind. Electron.*, vol. 64, no. 9, pp. 7467-7477, Sept. 2017.

[8] V. Mariani, F. Vasca, J. C. Vásquez, and J. M. Guerrero, “Model Order Reductions for Stability Analysis of Islanded Microgrids With Droop Control,” *IEEE Trans. Ind. Electron.*, vol. 62, no. 7, pp. 4344-4354, July 2015.

[9] M. Huang, Y. Peng, C. K. Tse, Y. Liu, J. Sun, and X. Zha, “Bifurcation and Large-Signal Stability Analysis of Three-Phase Voltage Source Converter Under Grid Voltage Dips,” *IEEE Trans. Power Electron.*, vol. 32, no. 11, pp. 8868-8879, Nov. 2017.

[10] Y. Wang, X. Wang, F. Blaabjerg, and Z. Chen, “Harmonic Instability Assessment Using State-Space Modeling and Participation Analysis in Inverter-Fed Power Systems,” *IEEE Trans. Ind. Electron.*, vol. 64, no. 1, pp. 806-816, Jan. 2017.

[11] L. Meng and J. M. Guerrero, “Optimization for Customized Power Quality Service in Multibus Microgrids,” *IEEE Trans. Ind. Electron.*, vol. 64, no. 11, pp. 8767-8777, Nov. 2017.

[12] X. Guo, Z. Lu, B. Wang, X. Sun, L. Wang and J. M. Guerrero, “Dynamic Phasors-Based Modeling and Stability Analysis of Droop-Controlled Inverters for Microgrid Applications,” *IEEE Trans. Smart Grid*, vol. 5, no. 6, pp. 2980-2987, Nov. 2014.

[13] Q. Zhong, L. Lin, G. Wang, Y. Zhang and Z. Wu, “Harmonic analysis model for voltage source converter under unbalanced conditions,” *IET Gener. Transm. Distrib.*, vol. 9, no. 1, pp. 12-21, 1 8 2015.

[14] A. M. Stankovic, S. R. Sanders and T. Aydin, “Dynamic phasors in modeling and analysis of unbalanced polyphase AC machines,” *IEEE Trans. Energy Convers.*, vol. 17, no. 1, pp. 107-113, Mar 2002.

[15] H. Zhu, Z. Cai, H. Liu, Q. Qi, and Y. Ni, “Hybrid-model transient stability simulation using dynamic phasors based HVDC system model,” *Elect. Power Syst. Res.*, vol. 76, pp. 582–591, Apr. 2006.

[16] Z. Miao, L. Piyasinghe, J. Khazaei and L. Fan, “Dynamic Phasor-Based Modeling of Unbalanced Radial Distribution Systems,” *IEEE Trans. Power Syst.*, vol. 30, no. 6, pp. 3102-3109, Nov. 2015.

[17] K. Shuai, W. Huang, C. Shen, J. Ge, and J. Shen, “Characteristics and Restraining Method of Fast Transient Inrush Fault Currents in Synchronverters,” *IEEE Trans. Ind. Electron.*, vol. 64, no. 9, pp. 7487-7497, Sept. 2017.

[18] T. Yang, S. Bozhko, J. M. Le-Peuvedic, G. Asher and C. I. Hill, “Dynamic Phasor Modeling of Multi-Generator Variable Frequency Electrical Power Systems,” *IEEE Trans. Power Syst.*, vol. 31, no. 1, pp. 563-571, Jan. 2016.

[19] Q. C. Zhong, “Power-Electronics-Enabled Autonomous Power Systems: Architecture and Technical Routes,” *EEE Trans. Ind. Electron.*, vol. 64, no. 7, pp. 5907-5918, Jul. 2017.

This article has been accepted for publication in a future issue of this journal, but has not been fully edited. Content may change prior to final publication. Citation information: DOI 10.1109/TIE.2018.2844828, IEEE Transactions on Industrial Electronics

Zhikang Shuai (S'09-M'10-SM'17) received the B.S. and Ph.D. degree from the College of Electrical and Information Engineering, Hunan University, Changsha, China, in 2005 and 2011, respectively, all in electrical engineering. He was at Hunan University, as an Assistant Professor between 2009 and 2012, an Associate Professor in 2013, and a Professor in 2014. His research interests include power quality control, power electronics, and microgrid stability analysis and control.

Dr. Shuai is the Associate Editor of IEEE Journal of Emerging and Selected Topics in Power Electronics, CSEE Journal of Power and Energy Systems, Chinese Journal of Electrical Engineering. He received the 2010 National Scientific and Technological Awards of China, the 2012 Hunan Technological Invention Awards of China, and the 2007 Scientific and Technological Awards from the National Mechanical Industry Association of China.

Yelun Peng received the B.S. degree in electrical and information engineering from Changsha University of Science and Technology, Changsha, China, in 2013. He is currently pursuing the Ph.D. degree in electrical engineering at the college of electrical and information engineering from Hunan University, Changsha. In 2017, he was a guest Ph.D. student at the Department of Energy Technology, Aalborg University, Denmark. His research interests include modeling and stability analysis for the AC microgrid system.

Josep M. Guerrero (S'01-M'04-SM'08-FM'15) received the B.S. degree in telecommunications engineering, the M.S. degree in electronics engineering, and the Ph.D. degree in power electronics from the Technical University of Catalonia, Barcelona, in 1997, 2000 and 2003, respectively. Since 2011, he has been a Full Professor with the Department of Energy Technology, Aalborg University, Denmark, where he is responsible for the Microgrid Research Program (www.microgrids.et.aau.dk). From 2012 he is a guest Professor at the Chinese Academy of Science and the Nanjing University of Aeronautics and Astronautics; from 2014 he is chair Professor in Shandong University; from 2015 he is a distinguished guest Professor in Hunan University; and from 2016 he is a visiting professor fellow at Aston University, UK, and a guest Professor at the Nanjing University of Posts and Telecommunications.

His research interests is oriented to different microgrid aspects, including power electronics, distributed energy-storage systems, hierarchical and cooperative control, energy management systems, smart metering and the internet of things for AC/DC microgrid clusters and islanded minigrids; recently specially focused on maritime microgrids for electrical ships, vessels, ferries and seaports. Prof. Guerrero is an Associate Editor for the IEEE TRANSACTIONS ON POWER ELECTRONICS, the IEEE TRANSACTIONS ON INDUSTRIAL ELECTRONICS, and the IEEE Industrial Electronics Magazine, and an Editor for the IEEE TRANSACTIONS on SMART GRID and IEEE TRANSACTIONS on ENERGY CONVERSION. He has been Guest Editor of the IEEE TRANSACTIONS ON POWER ELECTRONICS Special Issues: Power Electronics for Wind Energy Conversion and Power Electronics for Microgrids; the IEEE TRANSACTIONS ON INDUSTRIAL ELECTRONICS Special Sections: Uninterruptible Power Supplies systems, Renewable Energy Systems, Distributed Generation and Microgrids, and Industrial Applications and Implementation Issues of the Kalman Filter; the IEEE TRANSACTIONS on SMART GRID Special Issues: Smart DC Distribution Systems and Power Quality in Smart Grids; the IEEE TRANSACTIONS on ENERGY CONVERSION Special Issue on Energy Conversion in Next-generation Electric Ships. He was the chair of the Renewable Energy Systems Technical Committee of the IEEE Industrial Electronics Society. He received the best paper award of the IEEE Transactions on Energy Conversion for the period 2014-2015, and the best paper prize of IEEE-PES in 2015. As well, he received the best paper award of the Journal of Power Electronics in 2016. In 2014, 2015, and 2016 he was awarded by Thomson Reuters as Highly Cited Researcher, and in 2015 he was elevated as IEEE Fellow for his contributions on "distributed power systems and microgrids."

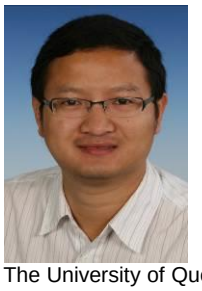

Yong Li (S'09–M'12–SM'14) was born in Henan, China, in 1982. He received the B.Sc. and Ph.D. degrees in 2004 and 2011, respectively, from the College of Electrical and Information Engineering, Hunan University, Changsha, China.

Since 2009, he worked as a Research Associate at the Institute of Energy Systems, Energy Efficiency, and Energy Economics (ie3), TU Dortmund University, Dortmund, Germany, where he received the second Ph. D. degree in June 2012. After then, he was a Research Fellow with The University of Queensland, Brisbane, Australia. Since 2014, he is a Full Professor of electrical engineering with Hunan University. His current research interests include power system stability analysis and control, ac/dc energy conversion systems and equipment, analysis and control of power quality, and HVDC and FACTS technologies.

Z. John Shen (S'89-M'94-SM'01-F'11) received BS from Tsinghua University, China, in 1987, and M.S. and Ph.D. degrees from Rensselaer Polytechnic Institute, Troy, NY, in 1991 and 1994, respectively, all in electrical engineering.

He was on faculty of the University of Michigan-Dearborn between 1999 and 2004, and the University of Central Florida between 2004 and 2012. He joined the Illinois Institute of Technology in 2013 as the Grainger Chair Professor in Electrical and Power Engineering. He has also held a courtesy professorship with Hunan University, China since 2007; and with Zhejiang University, China since 2013. His research interests include power electronics, and power semiconductor devices, etc.

Dr. Shen has been an active volunteer in the IEEE Power Electronics Society, and has served as VP of Products 2009-2012, Associate Editor and Guest Editor in Chief of IEEE Transactions on Power Electronics, technical program chair and general chair of several major IEEE conferences.